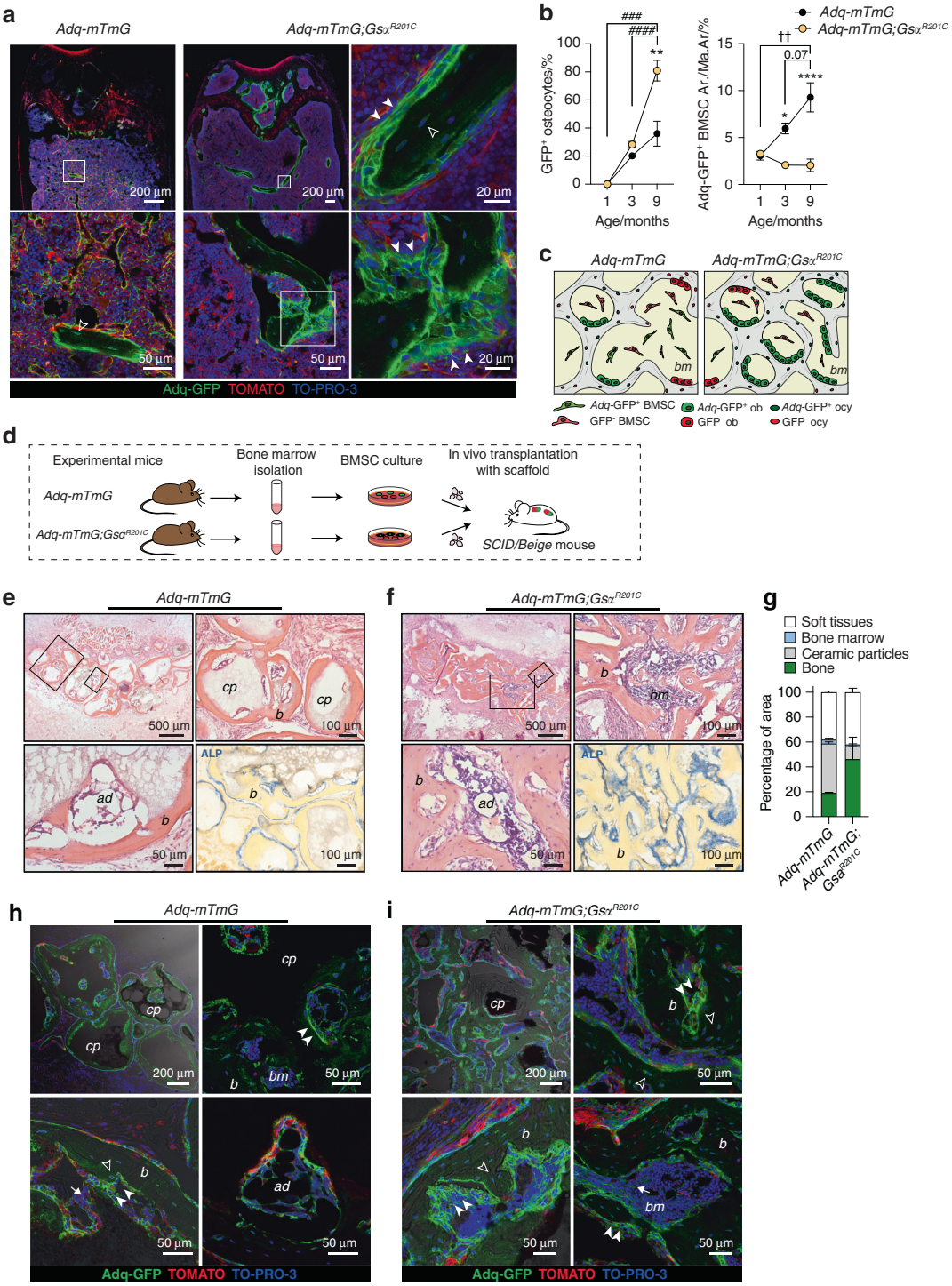

Fig. 4 Osteogenic activity of *Adq*-marrow stromal cells in situ and in heterotopic transplants. **a** Representative images of trabecular bone from 9-month-old *Adq-mTmG and Adq-mTmG;Gsα*^{R201C} mice showing GFP-marked osteoblasts (*arrowhead*) and osteocytes (*hollow arrowhead*). **b** Quantification of the fraction of GFP-labeled osteocytes and the GFP-labeled stromal cells area in *Adq-mTmG and Adq-mTmG;Gsα*^{R201C} mice at different ages. Statistical analysis performed using Two-way ANOVA followed by Sidak's multiple comparison test. $^{*}P < 0.05$, $^{**}P < 0.01$, $^{****}P < 0.000\ 1$ for comparison between *Adq-mTmG* and *Adq-mTmG;Gsα*^{R201C} mice. $^{\#\#\#}P < 0.001$, $^{\#\#\#\#}P < 0.000\ 1$ for comparison of different ages in *Adq-mTmG;Gsα*^{R201C} mice. $^{\dagger\dagger}P < 0.01$, for comparison of different ages in *Adq-mTmG* mice. The exact *P*-value was reported for the comparison between 3 and 9 months in *Adq-mTmG* mice. **c** Scheme of changes in the trabecular bone mass and GFP-labeled osteoblasts, osteocytes and stromal cells in *Adq-mTmG* and *Adq-mTmG;Gsα*^{R201C} mice. **d** Experimental design for the heterotopic transplantation of BMSCs in SCID/beige mice. **e**, **f** H&E-stained section of transplants made with BMSCs derived from *Adq-mTmG* (**e**) and *Adq-mTmG;Gsα*^{R201C} (**f**) mice, showing newly generated bone (*b*), bone marrow (*bm*) and adipocytes (*ad*). Carrier particles (*cp*) were easily recognized only in *Adq-mTmG* samples. Numerous ALP positive stromal cells were detected in transplants generated with cells from *Adq-mTmG;Gsα*^{R201C} mice. **g** Quantification of fraction of transplant area occupied by soft tissue, bone marrow, ceramic particles and bone. **h**, **i** Representative confocal images of the same transplants showing GFP labeling in the majority of osteoblasts (*arrowhead*) and osteocytes (*hollow arrowhead*), in adipocytes (*ad*) and in stromal cells (*arrow*)

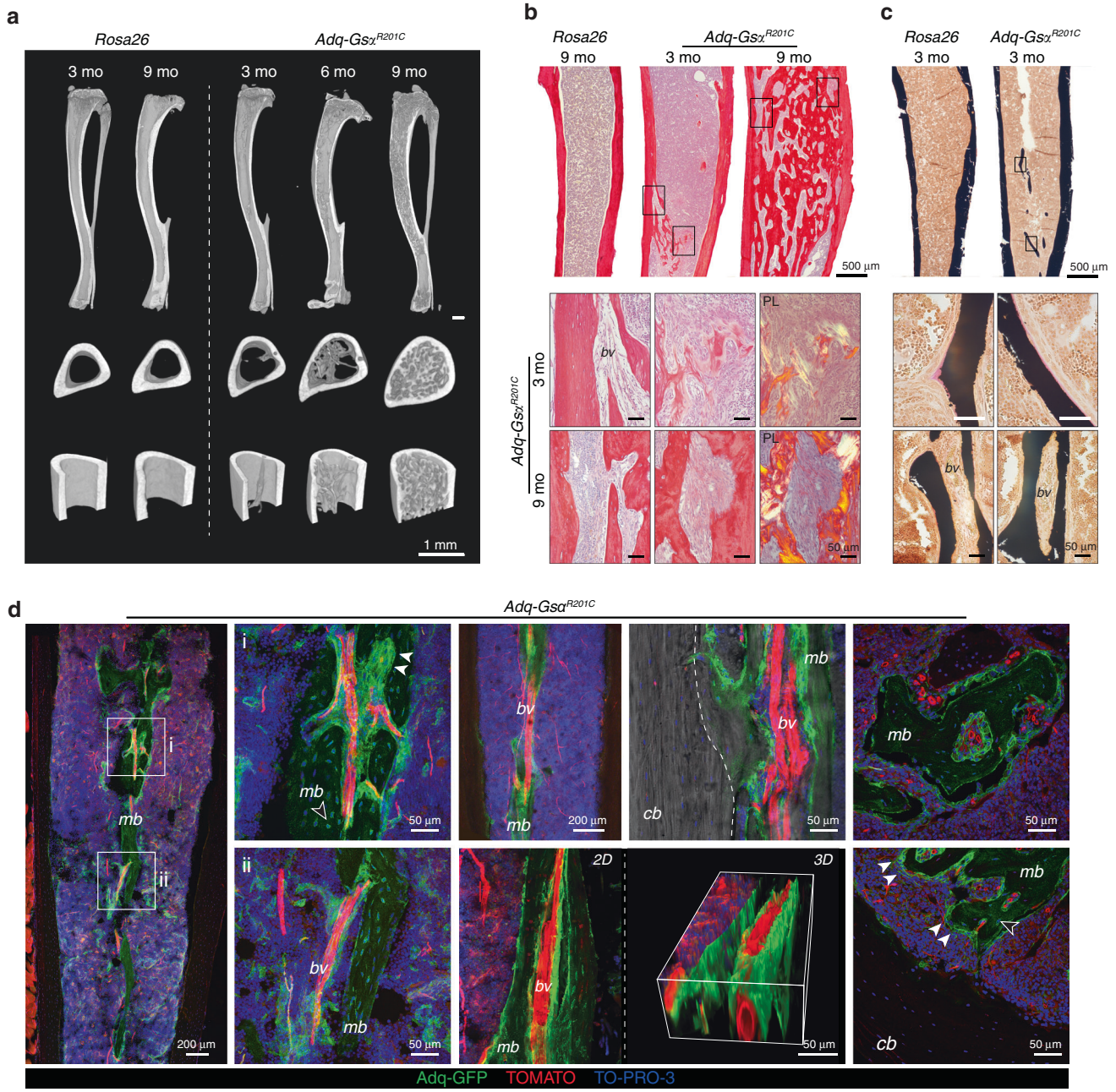

Fig. 5 Diaphyseal intramedullary bone formation in female *Adq-Gsα*^{R201C} mice. **a** Representative micro-computed tomography images of mice at different ages, showing the appearance and progression of the diaphyseal intramedullary bone. Transverse images were taken 2 mm above the tibia-fibular junction. **b** Transmitted and polarized (PL) light microscopy views of Sirius red stained sections of the tibial midshafts showing the appearance of the intramedullary bone in *Adq-Gsα*^{R201C} mice at 3 months of age and its subsequent expansion with obliteration of the medullary canal at older ages. PL shows the mixed woven and lamellar bone structure. **c** Von Kossa/Van Gieson stained MMA sections of undecalcified tibial midshafts showing mineralized intramedullary bone with a thin layer of osteoid rimmed with osteoblasts. **d** Representative images from confocal microscopy, showing medullary bone (*mb*) distributed around marrow blood vessels (*bv*) and its focal connection with cortical bone (*cb, dotted line*). GFP expression was observed in osteoblasts (*arrowhead*) and osteocytes (*hollow arrowhead*). 3D reconstruction was performed on a 50 µm-thick section using ImageJ software

cavity (Fig. 6b–d) similarly to what was observed in untreated female mice bearing the same genotype (Fig. 5). The origin of the intramedullary bone was explored in the tibiae and femora of E2-treated *Adq-mTmG;Gsα*^{R201C} male reporter mice, in which it included only GFP positive osteoblasts and osteocytes (Fig. 6e–g). After E2 treatment, an increase in the radiodensity of the metaphysis of long bones was detected in all male mice independent of their genotype (Fig. 6b, c). Histomorphometric analyses of trabecular bone demonstrated that BV/TV (Fig S6a) and osteoblast parameters **(**Fig S6b) were significantly higher in *Adq-Gsα*^{R201C} mice upon E2 treatment compared with Veh-treated *Adq-Gsα*^{R201C} and E2-treated control mice, in the absence of significant changes in osteoclast parameters (Fig S6c).

Osteogenic Adq-cells are not found in all skeletal segments

As observed in control *Adq-mTmG* mice, the expression of GFP in trabecular osteoblasts and osteocytes was never detected in the tail vertebrae of *Adq-mTmG;Gsα*^{R201C} mice (Fig. S1e, Fig. 7a).

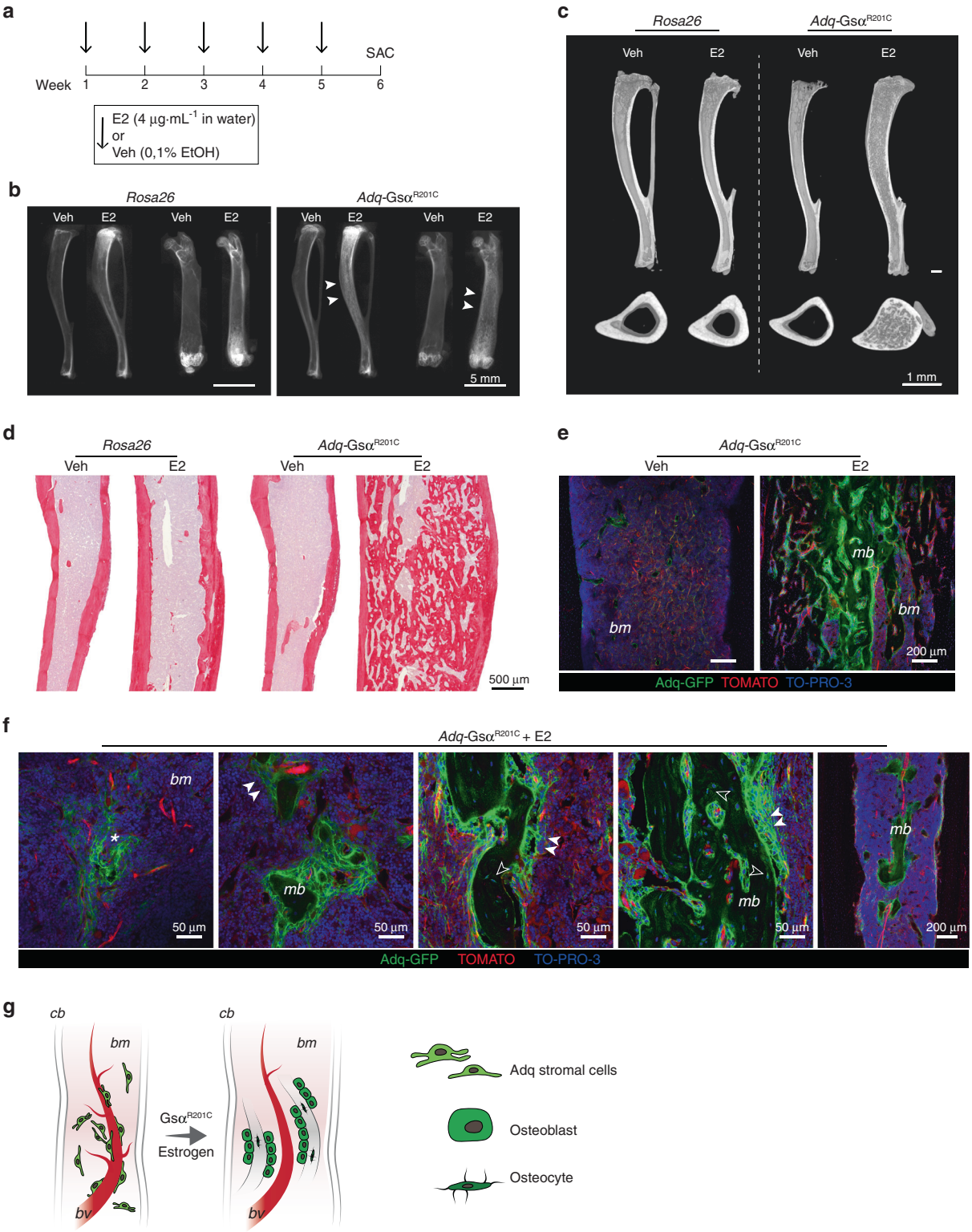

Fig. 6 Diaphyseal intramedullary bone formation is reproduced in *Adq-Gsα^{R201C}* male mice by 17β-estradiol (E2) treatment. **a** Experimental scheme of E2 treatment started at 5 months of age. **b** Radiographs of dissected tibiae and femora at the end of E2 treatment. Arrowheads indicate the increased density in the diaphyseal region of E2-treated bone segments from *Adq-Gsα^{R201C}* mice. **c** Representative longitudinal and transverse micro-CT images of Veh- and E2-treated mice, showing the diaphyseal intramedullary bone in E2-treated *Adq-Gsα^{R201C}* male mice. Transversal images were taken 2 mm above the tibia-fibular junction. **d** Sirius red stained sections of the tibial midshafts showing intramedullary bone in *Adq-Gsα^{R201C}* male mice after 6 weeks of E2 treatment. **e** Representative confocal images showing GFP-labeled intramedullary bone in E2-treated *Adq-Gsα^{R201C}* male mice. No bone is observed in Veh-treated mice. **f** Cluster of perivascular GFP-labeled stromal cells (*asterisk*) preceding the appearance of bone with GFP-labeled osteoblasts (*arrowhead*) and osteocytes (*hollow arrowhead*) in the marrow cavity of E2-treated *Adq-Gsα^{R201C}* mice. **g** Schematic representation of GFP-labeled medullary bone formation by *Adq-Gsα^{R201C}* marrow perivascular/stromal cells. *mb* Medullary bone, *bm* Bone marrow, *cb* Cortical bone, *bv* Blood vessel

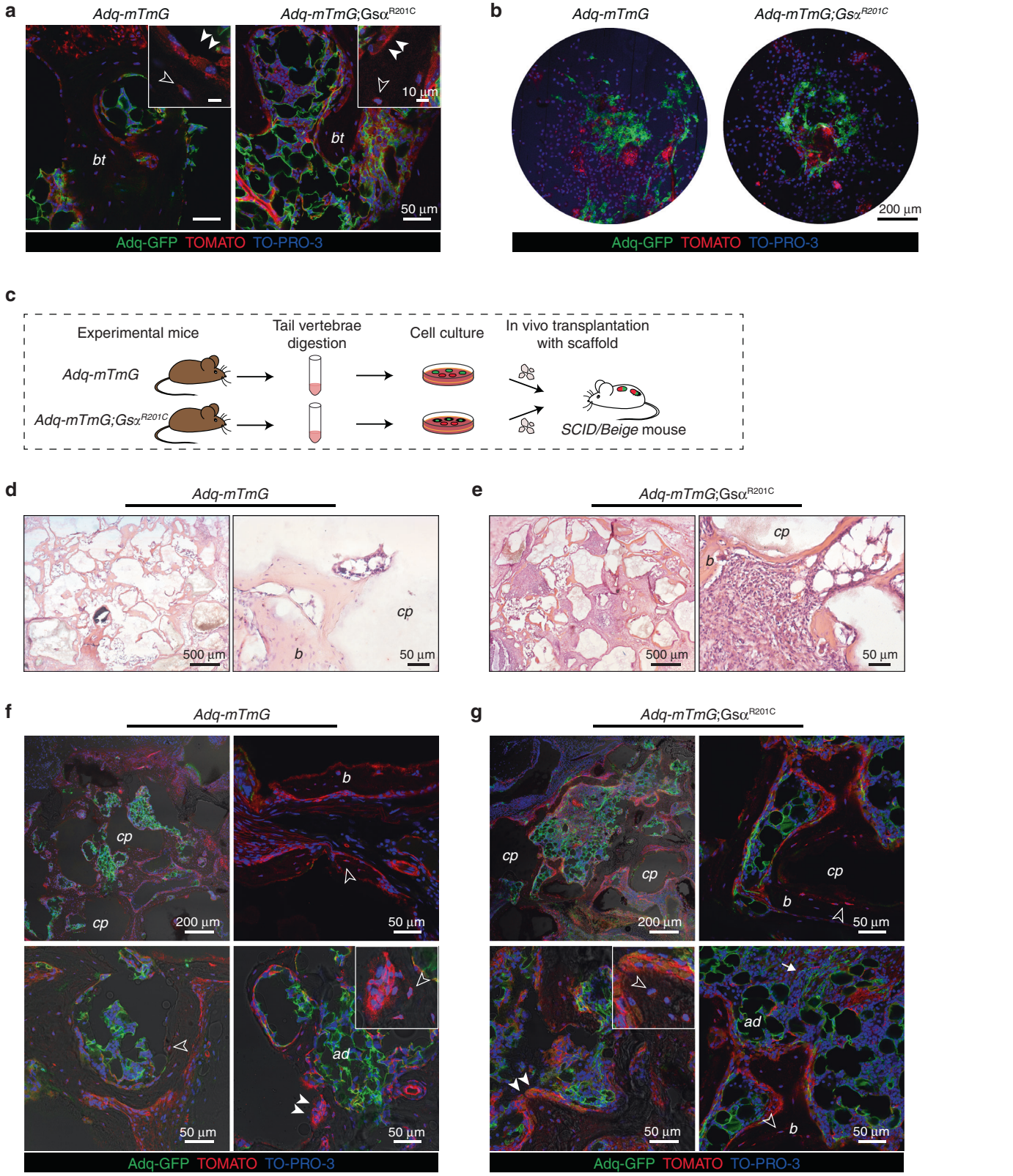

Fig. 7 *Adq*-marrow stromal cells from tail vertebrae are not osteogenic. **a**, Representative confocal microscopy images of bone trabeculae (*bt*) in the tail vertebrae of *Adq-mTmG* and *Adq-mTmG;Gsα^{R201C}* mice showing only Tomato positive osteoblasts (*arrowhead*) and osteocytes (*hollow arrowhead*). **b** GFP-labeled adherent cells in BMSC cultures isolated from tail vertebrae of 2-month-old mice. **c** Experimental design for the heterotopic transplantation of bone marrow stromal cells isolated from tail vertebrae. **d**, **e** Representative transmitted light microscopy images of *Adq-mTmG* and *Adq-mTmG;Gsα^{R201C}* transplants showing newly formed bone on the surfaces of carrier particles and inter-particle spaces occupied by bone marrow and adipocytes. **f**, **g** Representative confocal microscopy images of the same transplants showing GFP labeling in adipocytes (*ad*) and stromal cells (*arrow*) within the inter-particle spaces. Only Tomato positive osteoblasts (*arrowhead*) and osteocytes (*hollow arrowhead*) were found in these transplants. *b* Bone, *cp* Carrier particles